Characteristics of turbulent core-annular flows in a vertical pipe

Kiyoung Kim
Department of Mechanical & Aerospace Engineering
Seoul National University
Seoul 151-744, Korea
kky416@snu.ac.kr

Haecheon Choi
Department of Mechanical & Aerospace Engineering
Seoul National University
Seoul 151-744, Korea
choi@snu.ac.kr

ABSTRACT

The core-annular flow has been considered as a useful tool to effectively transport highly viscous oil by having lower viscous fluid such as water near the pipe surface. In the present study, we simulate turbulent core-annular flows by using a level-set method for tracking the phase interface between oil and water. A few different volume flow rate ratios are considered in a vertical pipe. Results show that the oil core region is nearly a plug flow and the water region is a turbulent flow. The phase interface between oil and water has waves with different wavenumbers and amplitudes which affect turbulent structures in water flow.

INTRODUCTION

Heavy oil reserves are estimated in 3 trillion barrels throughout the world, and this is about 15% of whole oil reserves (Oilfield review, 2006). However, heavy oil production needs much more capital and energy compare to the that of conventional oil because of low mobility due to its high viscosity. Although it has various properties in the presence of components such as asphaltenes, heavy metals, sulphur, heavy oil is usually defined to have the density of $\rho \approx 990$ kg/m^3 and viscosity of $\mu \approx 100$ kg/m·s at 25^{o}c (Joseph et al., 1997). It is almost impossible to transport the heavy oil in pipeline considering the high viscosity. Therefore, drag reduction technology is required in energy saving point of view.

There are several ways to reduce the drag such as provision of heating arrangements or addition of light oil. However, they require additional costs. The water lubricated transport is the one of the promising tool to reduce the drag. This arrangement is usually called 'core-annular flow' because one fluid is encapsulated in pipe core region by another fluid. In heavy oil and water flow, water is in annular region and oil is in a core region, so low viscous water can transport heavy oil efficiently.

Several studies have been conducted to investigate core-annular flows so far. Most of experimental studies have focused on flow types or global quantities such as the pressure drop (Oliemens *et al*., 1987; Bai *et al*., 1992; Prada and Bannwart, 2001; Rodrigues *et al*., 2009), whereas theoretical studies have considered only simple laminar flows (Hu and Joseph, 1989; Joseph and Renardy, 1993). Numerical studies have also been conducted recently, but they have been limited to laminar flows (Li and Renardy, 1999) or turbulent flow with deformable solid core using a turbulence model (Ko *et al.*, 2002).

In the present study, we conduct direct numerical simulations of turbulent core-annular flow by solving the unsteady three-dimensional Navier-Stokes and level-set equations in a vertical pipe (Fig. 1). We present the flow statistics and examine the phase interface waves.

NUMERICAL METHODS

The governing equations for the unsteady incompressible two-phase flow are given as

$$\frac{\partial(\rho u_i)}{\partial t} + \frac{\partial(\rho u_i u_j)}{\partial x_j} \tag{1}$$

$$= -\frac{\partial p}{\partial x_i} + \frac{\partial}{\partial x_j}\left(\mu\left(\frac{\partial u_i}{\partial x_j} + \frac{\partial u_j}{\partial x_i}\right)\right) + \rho g_i + \sigma\kappa\delta_i,$$

$$\frac{\partial u_i}{\partial x_i} = 0, \tag{2}$$

where x_i's are the cylindrical coordinates, u_i's are the corresponding velocity components, p is the pressure, g_i is the gravitational acceleration vector acting vertically, σ is the surface tension coefficient, κ is the curvature, and δ_i is the delta function which is unity at the phase interface and zero elsewhere. The ρ and μ are the density and viscosity of fluids defined in whole domain as given in the below:

Table 1. Flow conditions, domain sizes and number of grid points

Case	Initial Q_w/Q_o	Final Q_w/Q_o	Domain size (L_x, L_r, L_θ)	Grid (N_x, N_r, N_θ)
1	0.05	0.08	π×1×2π	128×49×1024
2	0.1	0.17	2π×1×2π	128×65×1024
3	0.2	0.36	3π×1×2π	256×97×1024
4	0.3	0.54	4π×1×2π	256×129×1024
5	0.4	0.73	4π×1×2π	256×145×1024

$$\rho = \rho_o + (\rho_w - \rho_o)\, H(\varphi) \qquad (3)$$

$$\mu = \mu_o + (\mu_w - \mu_o)\, H(\varphi). \qquad (4)$$

Here, the subscripts '*o*' and '*w*' denote oil and water, respectively, and $H(\varphi)$ is the heavy side function changing the value at the phase interface. The density and viscosity of oil are ρ_o = 963 $kg{\cdot}m^{-3}$ and μ_o = 17.6 $Pa{\cdot}s$, and those of water are ρ_w = 998 $kg{\cdot}m^{-3}$ and μ_w = 0.001 $Pa{\cdot}s$, respectively (Prada and Bannwart, 2001). The mean pressure gradient is set to be 400 Pa/m and corresponding Reynolds number based on the water property is $Re = \rho_w u_\tau R/\mu_w = 720$. All variables are non-dimensionalized by the pipe radius (R) and the friction velocity (u_τ).

A finite volume method with the second-order central difference scheme is used for spatial discretization and the second-order Crank-Nicolson method is used for temporal discretization except the surface tension force for which the explicit Euler method is used. The Newton iteration method with approximate factorization (Choi *et al.*, 1992) and Aitken type accelerator (Irons and Tuck, 1969) is adopted to solve the system matrix. The continuum surface force model is used for the surface tension (Brackbill *et al.*, 1992).

The level-set method is adopted for tracking the phase interface (Herrmann, 2008):

$$\frac{\partial \varphi}{\partial t} + u_j \frac{\partial \varphi}{x_j} = 0, \qquad (5)$$

where φ is the level-set function. A third-order TVD Runge-Kutta method and 5th-order WENO scheme are used for temporal and spatial discretizations, respectively.

Table 1 shows the flow conditions, computational domain sizes, and number of grid points. Uniform grids are used in the streamwise and azimuthal directions, while non-uniform grids are used in the radial direction. The

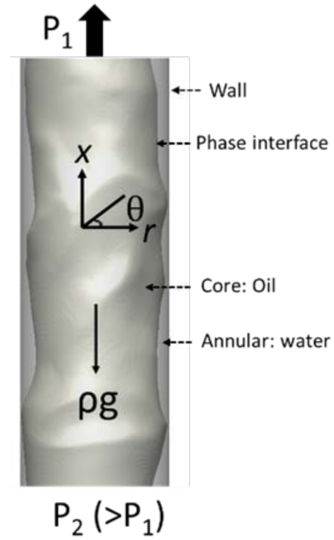

Figure 1. Schematic diagram of core-annular flow

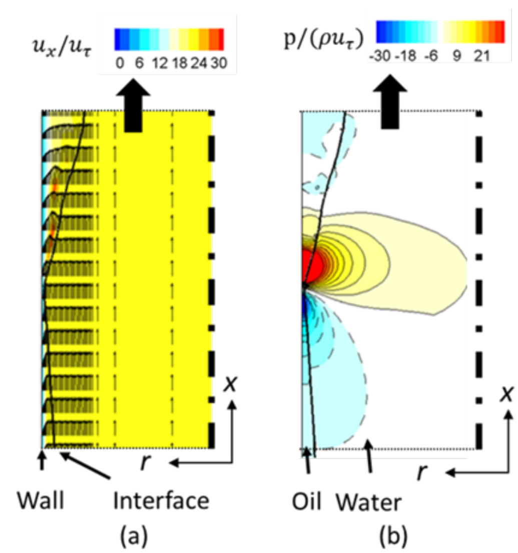

Figure 2. Instantaneous flow fields: (a) streamwise velocity with velocity vector; (b) pressure fluctuations

grid spacings in wall unit are $\Delta x^+ \approx$ 17~35, $\Delta r^+ \approx$ 0.12~0.22 and $\Delta R\theta^+ \approx 4.4$. Although the streamwise grid spacing is large compared to that used for single phase turbulent flow, it is enough to capture small eddies because the present flows are hard to evolve to a fully developed turbulent one due to the obstruction by the phase interface waves. The periodic boundary condition is applied for the streamwise and azimuthal diriections, and no-slip condition is used for the pipe wall.

During the simulations, we fix a constant mean pressure gradient to drive a flow inside the pipe and thus the mass (or volume) flow rates of oil and water change in

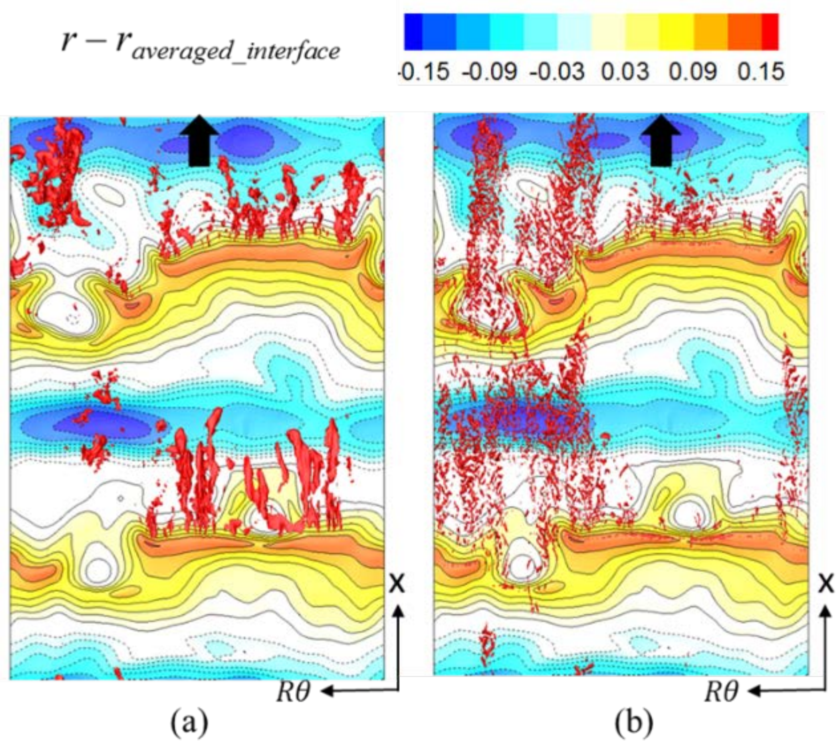

Figure 3. Instantaneous fields in a unfolded domain with the contour of relative height of phase interface to the averaged phase interface height : (a) isosurface of relative streamwise velocity to the core, $(u_\tau\text{-}u_{averaged\_core})^+ = 3$; (b)vortical structures represented by isosurfaces of $\lambda_2 = -500000$.

time. Initially, we provide five different volume flow rate ratios (Q_w/Q_o, where Q_w and Q_o are the volume flow rates of water and oil, respectively) by prescribing the velocity profiles of oil and water, but Q_w/Q_o changes in time and converges to another value because the velocities in water and oil vary in time under the constant mean pressure gradient.

RESULTS AND DISCUSSION

Flow Characteristics

The oil in core region and water in annular region flow differently because of the viscosity difference (Fig. 2 (a)). The annular region is turbulent flow and is affected by the phase interface shape. On the other hand, the core region is almost a plug flow due to the high viscosity and has small fluctuations (about 1% of the core bulk velocity). The fluctuations in core region are generated near the phase interface by fluctuated annular flow, but they rapidly decay in pipe center region. For this reason, early researchers who simulated the core-annular flow assumed that the core is deformable solid (Bai *et al.*, 1996).

Figure 2 (b) shows the pressure fluctuations near the phase interface crest. The crest is the location of phase interface closest to the wall. The pressure is maximum in front of crest and minimum behind it. As oil core is faster than water, there is the stagnation point at the windward side, so the pressure peak appears there. This is also observed in periodic hill flows (Frőhilch *et al.*, 2005). In this flow, the hill shape is very similar to the present phase interface geometry, but very thin gap ($\Delta r^+ \approx 20$) in core-annular flow produces a large difference between the maximum and minimum pressures with flow compression and expansion.

We unfold the cylindrical domain to a rectangle one and observe the water flow (Fig. 3). The contours are the heights of the phase interface relative to the averaged phase interface height. The windward side of the phase interface pushes water upward and hinders water from going downward (Fig. 3 (a)). The high crest plays a role as an obstacle and the small gap between the wall and phase interface attenuates the turbulence intensity. On the other hand, water can flow in the low crest region more easily, and vortical structures evolve there in the streamwise direction (Fig. 3 (b)). The flow separates when it passes through the crest because of the negative slope behind the crest.

Flow Statistics

Figure 4 shows the mean streamwise velocity of water flow. The velocity increases rapidly from the wall and shows almost flat profile when $(1\text{-}r)^+ > 60$ except the

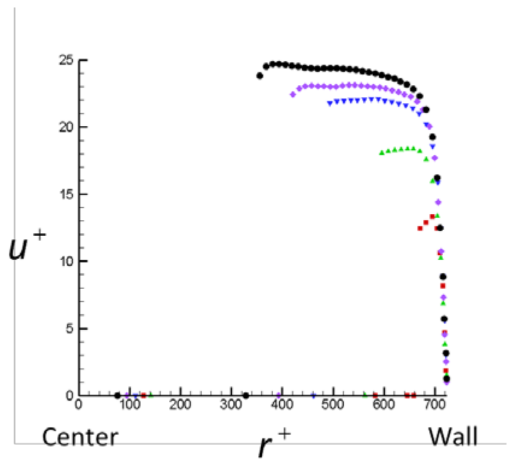

Figure 4. Mean streamwise water velocity for different volume flow rate ratios: ■, Q_w/Q_o ~ 0.08; ▲, 0.17; ▼ ,0.36; ◆, 0.54; ●, 0.73.

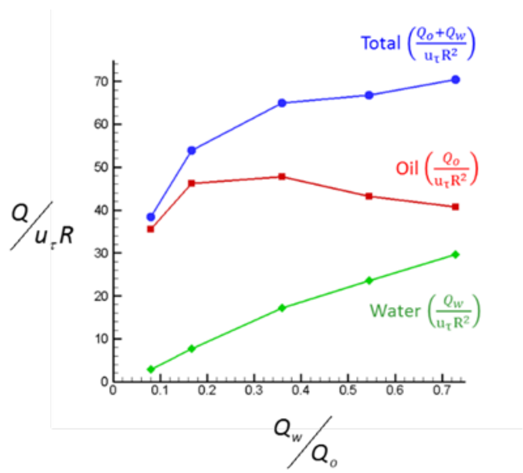

Figure 5. Volume flow rates of oil and water and their sum with Q_w/Q_o: ◆, water; ■, oil; ●, total.

case of Q_w/Q_o ~ 0.08 which has very narrow annular flow. This is because oil core flow has nearly constant velocity profile and drives water flow near the oil-water interface. The maximum mean water velocity increases with increasing the volume flow rate ratio, but the rate of change decreases.

Figure 5 shows the variations of the volume flow rate of each fluid with the volume flow rate ratio. It is interesting to note that the oil volume flow rate Q_o increases with increasing Q_w/Q_o, becomes maximum and then decreases. At low Q_w/Q_o, Q_o is lower than the maximum because the water region is so narrow that oil core is directly affected by the high viscous stress near the wall. On the other hand, at high Q_w/Q_o, Q_o is lower than the maximum because the oil area is reduced. The instantaneous flow fields are investigated for Q_w/Q_o ~ 0.36 at which the oil volume flow rate is maximum.

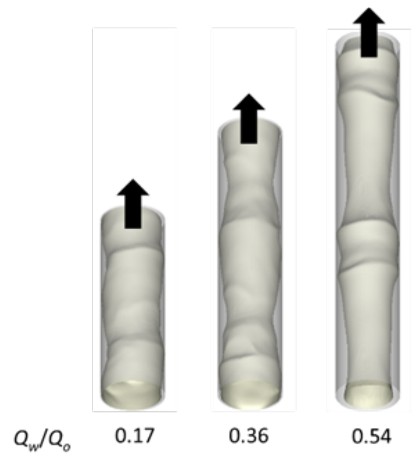

Figure 6. Phase interface waves for different volume flow rate ratios.

Wave dynamics

The large viscosity difference between oil and water makes the phase interface unstable and produces a wide spectrum of the wave. Owing to the instability of the phase interface, it is difficult to maintain the oil-in-core and water-in-annular arrangement which is a necessary condition for the efficient transport. Figure 6 shows the instantaneous phase interface shapes. The phase interface has waves consisting of different wavenumbers in the streamwise and azimuthal directions. The phase interface wave length and amplitude increase with increasing volume flow rate ratio.

Drag reduction

When we consider heavy oil without water (single-phase flow) at the same pressure gradient, the volume flow rate of oil is $Q/u_\tau R^2$ = 2.35 × 10^{-10} which is much less than core-annular flow, $Q/u_\tau R^2$ ~ $O(40)$. So, it is impossible to transport without water. Therefore it is evident that core-annular flow is an effective tool to transport high viscous heavy oil.

CONCLUSIONS

In the present study, we conducted direct numerical simulations of turbulent core-annular flow of heavy oil and water. Results showed that the core region is nearly a plug flow and the water region is turbulent flow. The water flow is affected by the phase interface shape. There is maximum oil flow rate condition which is the most efficient transport condition.

ACKNOWLEDGMENTS

This work is supported by the NRF programs (No. 2012M2A8A4055647) of MSIP, Korea. The computation time was provided by the Supercpmputing Center/Korea Institute of Science and Technology Information with supercomputing resources including technical support (KSC-2014-C2-044).

REFERENCES

Bai, R., Chen, K., Joseph, D. D., 1992, "Lubricated pipelining: stability of core-annular flow. Part 5. Experiments and comparison with theory", *Journal of Fluid Mechanics*, Vol. 240, pp. 97-132.

Bai, R. , Kelkar, K., Joseph, D. D., 1996, "Direct simulation of interfacial waves in a high-viscosity-ratio and axisymmetric core-annular flow", *Journal of Fluid Mechanics*, Vol. 327, pp.1-34.

Brackbill, J. U., Kothe, D. B., Zemach, C., 1992, "A continuum method for modeling surface tension", *Journal of Computational Physics*, Vol. 100, pp.335-354.

Choi, H., Moin, P., Kim, J., 1992, "Turbulent drag reduction: studies of feedback control and flow over riblets", *Rep.* TF-55, Department of Mechanical Engineering, Stanford University.

Feng, J., Huang, P. Y., Joseph, D. D., "Dynamics simulation of the motion of capsules in pipelines", 1995, *Journal of Fluid Mechanics*, Vol. 286, pp. 201-227.

Frőhlich, J. Mellen, C. P., Rodi, W., Temmerman, L., Leschziner, M. A., 2005, "Highly resolved large-eddy simulation of separated flow in a channel with streamwise periodic constrictions", *Journal of Fluid Mechanics*, Vol. 523, pp. 19-66.

Herrmann, M., 2008, "A balanced force refined level set grid method for two-phase flows on unstructured flow solver grids", *Journal of Computational Physics*, Vol. 227, pp. 2674-2706.

Hu, H. H., Joseph, D. D., 1989, "Lubricated pipelining: stability of core-annular flow. Part 2", *Journal of Fluid Mechanics*, Vol. 205, pp. 359–396.

Irons, B., Tuck, R. C., 1969, "A version of the Aitken accelerator for computer iteration", *International Journal of Numerical Methods in Engineering*, Vol. 1, pp. 275-277.

Joseph, D. D., Bai, R., Chen, K. P., Renardy, Y. Y., 1997, "Core-Annular flows", *Annual Review of Fluid Mechanics*, Vol. 29, pp. 65-90.

Joseph, D. D., Renardy, Y. Y., 1993, "Fundamentals of Two-Fluid Dynamics", New York: Springer-Verlag.

Ko, T., Choi, H. G., Bai, R., Joseph, D. D., 2002, "Finite element method simulation of turbulent wavy core-annular flows using a k-ω turbulence model method", *International Journal of Multiphase Flow*, Vol. 28, pp.1205-1222.

Li, J., Renardy, Y., 1999, "Direct simulation of unsteady axisymmetric core-annular flow with high viscosity ratio", *Journal of Fluid Mechanics*, Vol. 391, pp. 123-149.

Oliemans, R. V. A., Ooms, G., Wu, H. L., Duijvestijn, A., 1987, "Core annular oil/water flow: the turbulent-lubricating–film model and measurements in a 5 cm pipe loop", *International Journal of Multiphase Flow*, Vol. 13, pp. 23-31.

Ooms, R, Segal, A., Wees, A. V., Meerhoff, R., Oliemans, R. V. A., 1984, "A Theoretical model for core-annular flow of a very viscous oil core and a water annulus through a horizontal pipe", *International Journal of Multiphase Flow*, Vol. 10, pp. 41-60.

Prada, J. W. V., Bannwart, A. C., 2001, "Modeling of vertical core-annular flows and application to heavy oil production", *Journal of Energy Resource Technology*, Vol. 123, pp. 194-199.

Rodriguez, O. M. H., Bannwart, A. C., De Carvalho, C. H. M., 2009, "Pressure loss in core-annular flow: Modeling, experimental investigation and full-scale experiments", *Journal of Petroleum Science and Engineering*, Vol. 65, pp. 67-75.

Schlumberger, 2006 ,"Highlighting heavy oil", *Oilfield Review*, 2006 summer. pp. 34-35.